

# Mapping of Mineral Zones using the Spectral Feature Fitting Method in Jahazpur belt, Rajasthan, India

Ronak Jain<sup>1</sup>, Richa U Sharma<sup>2</sup>

<sup>1,2</sup>Indian Institute of Remote Sensing, 4- Kalidas Road, Indian Institute of Remote Sensing, ISRO, Dehradun – 248001, India

\*\*\*

**Abstract** - The main aim of this paper is to describe the Spectral Feature Fitting (SFF) Algorithm for the mineral mapping. Hyperspectral satellite imagery is having a high resolution which is more useful for the mineral identification and mapping and hence, capable to replacing the traditional techniques such as field-based approach and multispectral remote sensing for the mineral identification and classification. Pixels of the hyperspectral imagery contains the unique information about the materials present on the surface as it is having a high spectral resolution as well. Airborne hyperspectral imagery is having very high spectral as well as spatial resolution as compared to spaceborne hyperspectral imagery. Jahazpur belt area is in the southern part of the Jahazpur village of Bhilwara in Rajasthan. SFF has been applied to process Airborne Visible/Infrared Imaging Spectrometer Next Generation (AVIRIS-NG) imagery for identification and enhancement of the mineral mapping process with better accuracy. Minimum Noise Fraction (MNF) algorithm is used for the reduction of the dimensionality of the data. Pixel Purity Index (PPI) and n-Dimensional visualization for the extraction of the pure pixels (endmembers) from the cluster of pixels. That information is used for the classification with the help of the SFF algorithm. SFF method helps in the processing of imagery with high efficiency and preparing the mineral distribution map of the study area.

**Key Words:** AVIRIS-NG, Airborne-Hyperspectral imagery, Remote Sensing, Spectral Feature Fitting, Mineral mapping

## 1. INTRODUCTION

Remote Sensing is a expertise used for the data acquisition of the matters which are placed at distance or remote provinces and perform analysis for the interpretation (Sabins, 1999) of the physical characteristics of the attained data. Every object on the earth surface reflects or emits a certain amount of energy in the form of radiation and which is a part of electromagnetic radiation (EMR). Visible to microwave region of the EMR is used for the data acquisition in Remote Sensing (Gupta, 2003). Detection and mapping of the potential areas for mining and studying a different kind of mineralization are the very significant application of the remote sensing in the field of mineral exploration (Abbaszadeh & Hezarkhani, 2013; Sabine, 1999). This method can help to cover the huge areas on little cost as compared to other methods of exploration such as geophysical, geochemical and geological methods. Satellite imagery had been processed for a finding of the precise

location of the mineralized regions (hydrothermal alteration zones) connected to the metal mineralization by using various procedures such as Principal Component Analysis (PCA) and band ratio (Rajesh, 2004; Sabine, 1999).

Imaging spectroscopy is widely used by the scientist and researchers for the geologic mapping and mineral identification (Swayze et al., 1992). The availability of spaceborne Hyperspectral data is very limited. Satellite data is 0.4 – 2.5  $\mu\text{m}$  range. Therefore Airborne sensors (AVIRIS) are being used by the researchers for mineral mapping (Goetz & Srivastava, 1985; Kruse, Lefkoff, & Dietz, 1993; Kruse, 1988; Kruse, 2002; Kruse, Boardman, & Huntington, 2003). Airborne sensors provide the high spatial resolution (2-20 m), and high spectral resolution (10-20 nm) data for the various scientific domains (Kruse, 2002).

In this paper, Airborne Visible/Infrared Imaging Spectrometer Next Generation (AVIRIS-NG) data of the Jahazpur belt has been processed by using Spectral Feature Fitting (SFF) method. Now a day this algorithm is used for the spectral analysis of the imagery. The spectrum of the unknown pixel is used for the matching of the spectrum from the reference spectra for recognition of the similarities between both the spectrum (Van der Meer & De Jong, 2003)

## 2. STUDY AREA

The area is located between the latitude 25°26'34.80'' to 25°30'7.20'' in the North and longitude 75°10'22.80'' to 75°14'16.80'' in the East on the geological map of the Bhilwara prepared by the Geological Society of India. This area is in the south-eastern part of the Jahazpur city of Bhilwara district in Rajasthan, India. Ajmer and Tonk from north, Hindoli and Mandalgarh from the east, Kotri from south and Shahpura from west surrounded the Jahazpur city. The location of the study area is shown in Figure 1.

Jahazpur belt belongs to Jahazpur group of the Bhilwara Supergroup (BSG) and having an age of the lower Proterozoic. It is mainly important for the presence of minerals such as iron ore and dolomite. The trend of the Bhilwara Supergroup rocks is NNE-SSW. The basic lithology of the area consists of the dolomite, quartzites, banded iron formation (BIF) and conglomerates etc.

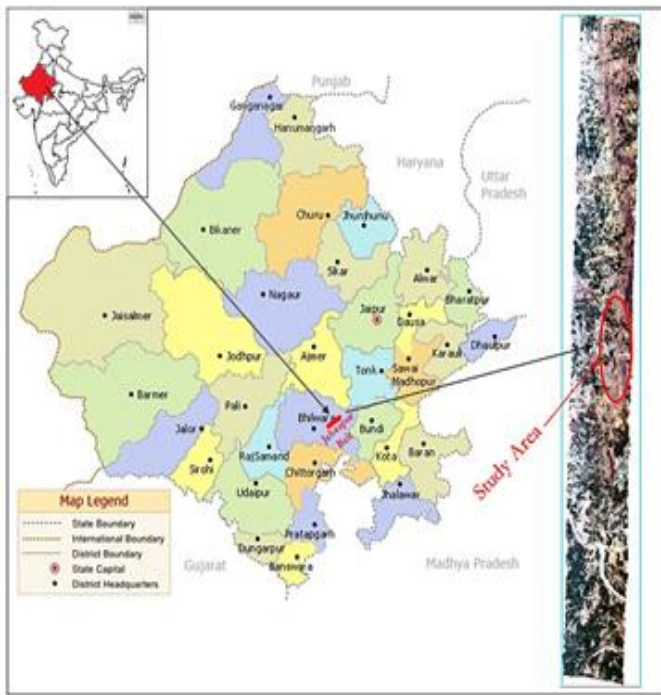


Figure 1: Location of the Study Area with AVIRIS-NG strip

The stratigraphic sequence of the Bhilwara Supergroup is given by Gupta et al., (1997). The stratigraphy of the study area of BSG is described in Table 1

Table 1: Stratigraphy of the Study Area. Source: (GSI, 2004)

Age	Supergroup	Group	Formation	Lithology
Lower Proterozoic	Bhilwara Supergroup	Jahazpur Group	Ummedpura Formation	Carbonaceous/purple phyllite Orthoquartzite Dolomite Grey phyllite (tuff) & dolomite with BIF Conglomerate/gritty quartzite
			Jawal Formation	Dolomite with BIF Conglomerate & gritty quartzite
Archean		Hindoli Group	Sujanpura Formation	Metagreywacke Phyllite ± garnet

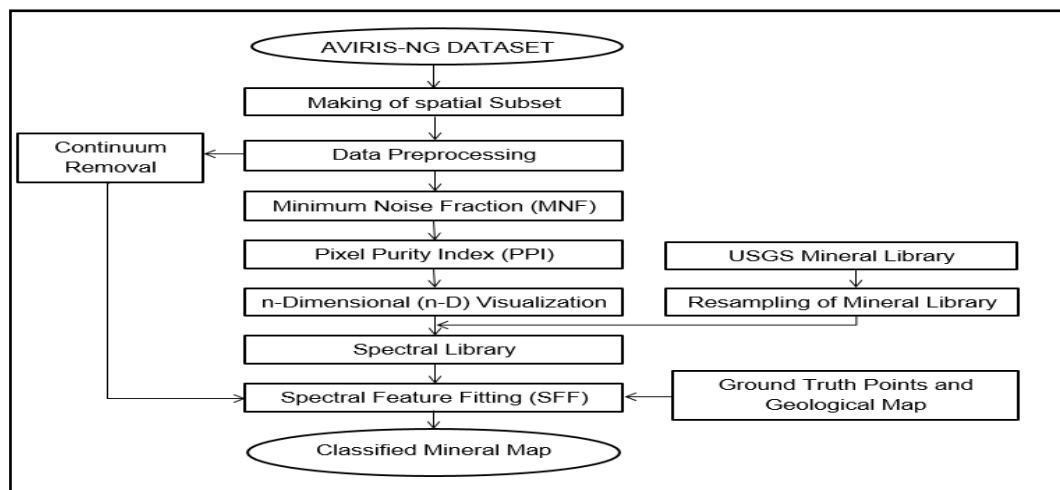


Figure 2: Overall Adopted Methodology

### 3. METHODOLOGY

The overall adopted methodology, algorithm and processing steps for these have been depicted in the given Figure 2.

The AVIRIS-NG data strip is too large to process at a single time so spatial subset from the data strip is extracted out for this study. For the making of spatial subset region of interest (ROI) tool is used.

#### 3.1 DATA PREPROCESSING

The AVIRIS-NG is a whisk broom sensor with 425 contiguous bands of narrow bandwidth. The presence of the huge amount of the spectral data and noise in the imagery, pre-processing of the data is required to manage the noise with high attention. Pre-processing of the data is the initial step. The AVIRIS-NG level L2 dataset is radiometrically and atmospherically corrected data. It requires the removal of the bad bands i.e. bands contain the noise and water vapour absorption bands. After the preprocessing 363 bands are remaining for the further processing.

#### 3.2 MINIMUM NOISE FRACTION (MNF)

The imagery of huge data volume generates a larger amount of data on processing and require higher complex computation i.e. dimensionality problem. Transformation of the high dimensional data (space) into low dimensional data (space) without losing the information is known as dimensionality reduction. To overcome the curse of data dimensionality and to improve the analytical accuracy, dimensionality reduction of the dataset is a must.

The approach used for the dimensionality reduction is Minimum Noise Fraction (MNF). Green et al., (1988) developed the MNF transform for ordering components in the form of image qualities. They had chosen a new component to adequately increase (maximize) the SNR and images are arranged with the increasing quality/decreasing noise. MNF effectively reduces the dimensionality of the dataset on the basis of noise statistics information and eliminate the noise. Shift difference method (nearest neighbour method) is used for the computation of the noise statistics given by Green et al., (1988).

### 3.3 PIXEL PURITY INDEX (PPI)

PPI is an automated procedure applied on the MNF components to trace the extremely pure spectra nearby to the boundaries of n-dimensional data cloud. Boardman, Kruse, & Green, (1995) proposed the procedure of PPI. PPI is a popular statistics technology (Van der Meer et al., 2012). It is extensively used for the extraction of endmembers from hyperspectral imagery. To find the spectrally pure (unique) pixels from the dataset, PPI algorithm plays an important role.

### 3.4 N-DIMENSIONAL VISUALIZATION

n-Dimensional (n-D) visualizer is an interactive technique for the extraction of the pure pixels (endmembers) spectra from the spectral mixing space (Boardman & Kruse, 2011). It allows the spinning of the pixels in the scatterplot in real time. According to Boardman, (1993), points to be considered as spectra in the n-dimensional scatterplot, n denotes the number of bands. For a pixel, the spectral reflectance or radiance (DN) values for every single band is given by n values of that points having coordinates in n-space. Amount of the spectrally pure endmembers and their spectral signatures are estimated on the basis of the points distribution in n-dimensional space (Boardman, 1993; Boardman & Kruse, 2011; Boardman et al., 1995).

### 3.5 SPECTRAL FEATURE FITTING (SFF)

Spectral analysis of the satellite imagery is done by using the various methods and algorithms. But the base of every method is to a comparison of each pixel spectrum of satellite imagery with the reference (known) spectrum. The main characteristics features and parameters to be considered are shape, position and strength of the absorption bands in the mineral's spectral diagram. Those are matched/fitted to the reference spectrum (Van der Meer, 2004). SFF algorithm gives better results in spectral analysis method for processing of the satellite imagery.

The Spectral Feature Fitting (SFF) algorithm eliminates the continuum of absorption feature from the spectra of the reference spectral library and also from each spectrum of the image dataset. The SFF compares the continuum removed spectrum of the image with the continuum removed spectrum of reference spectra and operated the least square fitting. The selection of the best

fitting material on the basis of spectral features or group of features is done by comparing the correlation coefficient of fits (Clark, Swayze, Boardman, & Kruse, 1993). Figure 3 illustrated the working procedure of SFF.

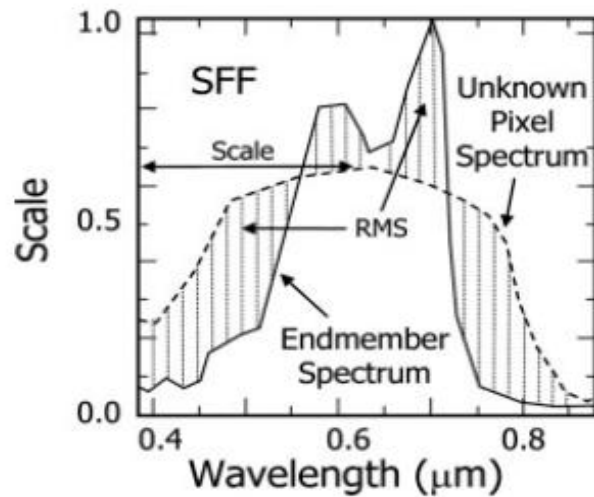


Figure 3: Working approach of Spectral Feature Fitting (SFF). Source: (Harris, 2006)

The process of feature extraction involved the first step as continuum removal which is used to identify the individual absorption features carrying the spectrum (Kruse, 1993). The convex hull using straight line segments are fitted on the top of the spectrum that joins the maxima of local spectra is known as a continuum. For removal of the continuum, original spectrum (S) for every pixel in an image is divided by the (C) continuum curve (Harris, 2017), as mentioned in equation 1:

$$S_{cr} = \frac{S}{C} \tag{1}$$

Where  $S_{cr}$  = Continuum-removed spectra, S = Original spectra, C = Continuum curve

Initially, subtraction of the continuum removed spectra by one is done to generate the Scale image which helps for the predictions, thus inverting spectra and continuum is made to zero. The scale is used for the determination of the depth of the absorption feature in each pixel. Scale factor represents the abundance of spectral features. Band by band calculation is performed for computation of least squares fit. Higher scale value represents the strong absorption in the mineral's spectral band. Mineral abundance is highly related to the scale value (Van der Meer, 2004; Verdel et al., 2001). Brighter pixels in the scale image represents better matching of the pixel spectrum from the reference spectrum of the mineral. RMS (Root Mean Square) error image is also produced for each endmember to compute the total RMS error. Low RMS pixels appear black (darker) in the image and their shape of the spectra is highly similar to the reference spectrum of the mineral. RMS is a method, which is used for the examination

of the existence and absence of the minerals (Van der Meer, 2004; Verdel et al., 2001). Those are having low RMS error and high scale factor are seems closely matched. An equal number of images are generated by the scale and RMS. The Fit images are generated by making a ratio between scale image and RMS error image to measure the similarities (match) between the unknown spectrum and reference spectrum on the basis of pixel-by-pixel (Van der Meer & De Jong, 2003).

#### 4. RESULTS

Continuum removed imagery is used for the SFF algorithm. It matches the continuum removed spectra of the reference mineral with the continuum removed spectra of the imagery. Fit images are generated as an output of SFF algorithm. Dolomite, iron, conglomerate (quartz, feldspar), talc, amphibolite (augite), vermiculite, clay (kaolinite, smectite - montmorillonite) etc. minerals are considered as reference minerals in the Jahazpur belt.

After processing of imagery iron (pyrrhotite, limonite), clay (montmorillonite, kaolinite), dolomite, quartz, vermiculite and talc minerals are mapped in the study area. Iron and dolomite minerals are the major minerals in the Jahazpur region. Fit images of every mineral are classified.

Minerals are divided into few groups. The first group is of clay minerals (Figure 4A), second is dolomite (Figure 4B), third is iron – pyrrhotite, limonite (Figure 4C), and last is other minerals – talc, quartz and vermiculite (Figure 4D). A separate map of minerals helps in the identification of the distribution of every mineral in the field. In the final step mineral map of the study area (Jahazpur belt, Bhilwara) is prepared. The final classified mineral map (Figure 5) is prepared by using the thresholding of all the minerals in ENVI software. This map indicates the main mineralized zones (dolomite and iron minerals) of the Jahazpur belt (study area) defining the threshold value. Resultant images are used for the preparation of the mineral distribution maps.

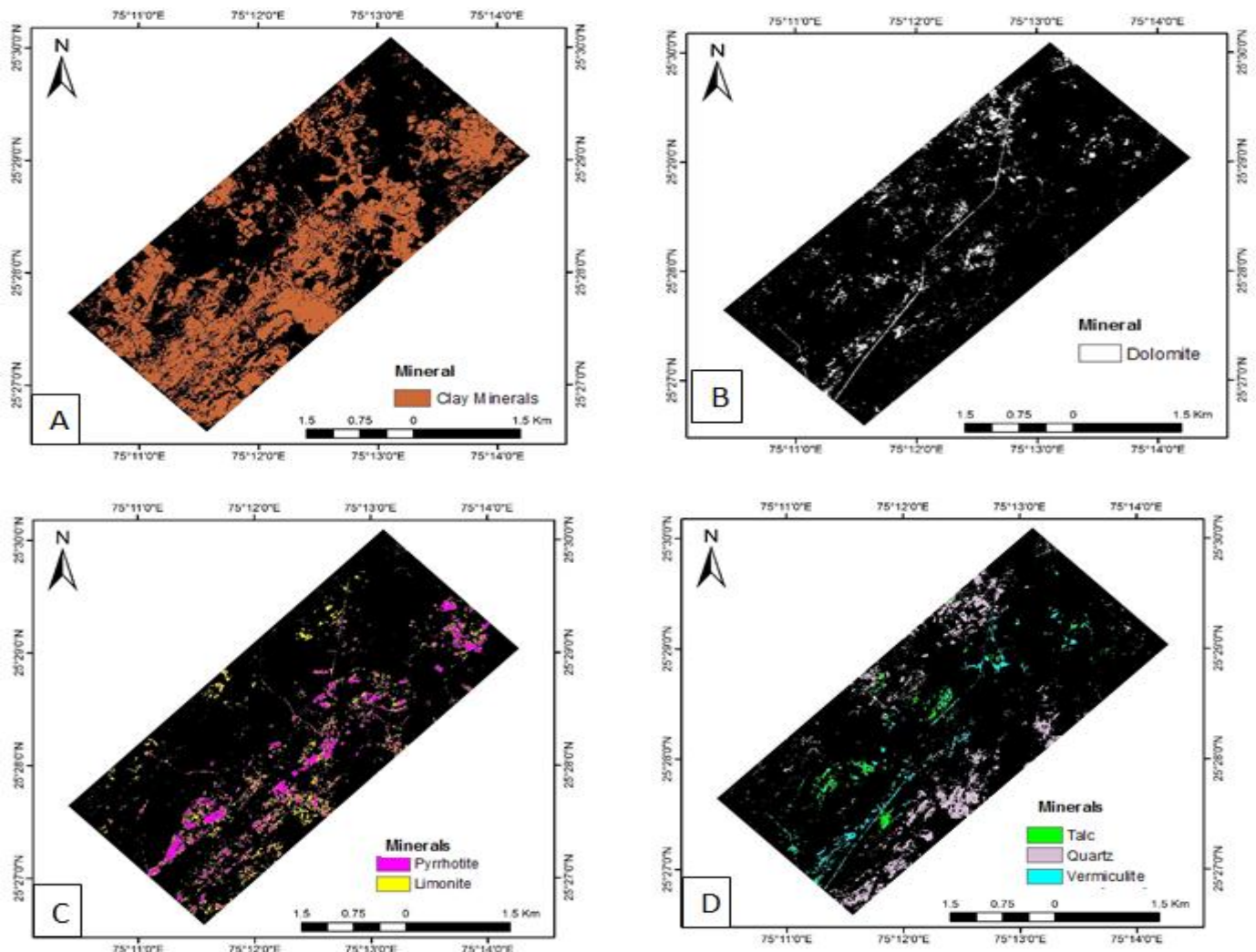


**Figure 4: Mineral distribution maps of the different minerals after applying the threshold values on the fit images generated by SFF algorithm. A: Clay minerals, B: Dolomite, C: Iron minerals (pyrrhotite & limonite), D: Other minerals (Talc, quartz & vermiculite).**

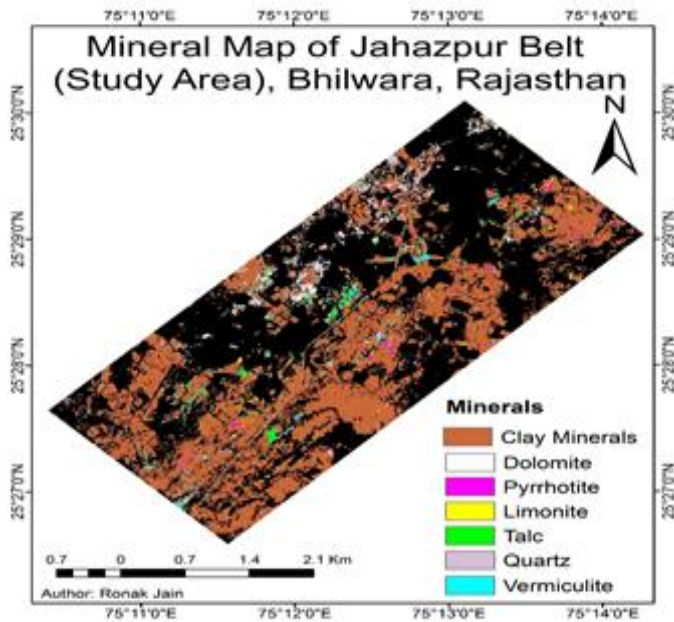


**Figure 5: Classified Mineral Map of the Jahazpur Belt (Study Area), Rajasthan**

## 5. CONCLUSIONS

Remote sensing is a powerful tool in the mineral mapping domain. It is a method of lower cost than the other methods such as geophysical and geochemical exploration method. AVIRIS-NG imagery is having very high spatial as well as a spectral resolution so highly useful for the mapping of the minerals, lithological units, and different regional structures. Spectral Feature Fitting (SFF) algorithm is used for the processing of the AVIRIS-NG imagery. Spectral absorption features are used for the identification of the minerals. Every mineral has a unique spectral absorption value. Identified minerals are mapped by Final mineral map of the area is prepared in the GIS environment having the SFF output maps. The resultant mineral map is presenting the effectiveness and capabilities of the SFF algorithm for the identification and mapping of the minerals.

The area mainly consists of the iron (pyrrhotite & limonite) and dolomite minerals. The maximum part of the study area is covered by the clay minerals. The clay mineral (smectite) also contains the iron. So, the region is highly useful for the exploration of iron and dolomite minerals.

Geological map of the region is having the different litho-assemblages. Those litho-assemblages validated the SFF classified mineral map. The mineral map is having the same trend of the mineral distribution as the lithological units are distributed into the area. So, the mineral distribution map of the region is accurate and highly useful for the mineral exploration.

These studies are confirming the capabilities of the remote sensing technique and SFF algorithm for the processing of the AVIRIS-NG imagery in the geological domain for mineral mapping.

## REFERENCES

- Abbaszadeh, M., & Hezarkhani, A. (2013). Enhancement of hydrothermal alteration zones using the spectral feature fitting method in Rabor area, Kerman, Iran. *Arabian Journal of Geosciences*, 6, 1957–1964. <https://doi.org/10.1007/s12517-011-0495-0>
- Boardman, J. W. (1993). Automating spectral unmixing of AVIRIS data using convex geometry concepts. In *JPL, Summaries of the 4th Annual JPL Airborne Geoscience Workshop. Volume 1: AVIRIS Workshop* (pp. 11–14). United States: JPL Publication.
- Boardman, J. W., & Kruse, F. A. (2011). Analysis of imaging spectrometer data using N-dimensional geometry and a mixture-tuned matched filtering approach. *IEEE Transactions on Geoscience and Remote Sensing*, 49(11), 4138–4152. <https://doi.org/10.1109/TGRS.2011.2161585>
- Boardman, J. W., Kruse, F. A., & Green, R. O. (1995). Mapping target signatures via partial unmixing of AVIRIS data. In *Summaries of the Fifth Annual JPL Airborne Earth Science Workshop. Volume 1: AVIRIS Workshop* (pp. 23–26). United States: JPL Publication.
- Clark, R. N., Swayze, G., Boardman, J., & Kruse, F. (1993). Comparison of Three methods for Material Identification and mapping. In *JPL, Summaries of the 4th Annual JPL Airborne Geoscience Workshop. Volume 1: AVIRIS Workshop* (pp. 31–33). United States: JPL Publication.
- Goetz, A. F. H., & Srivastava, V. (1985). Mineralogical mapping in the Cuprite Mining District, Nevada. In *Proceedings of the Airborne Imaging Spectrometer (AIS) Data Analysis Workshop, JPL, Publication 85-41* (pp. 22–29).
- Green, A. A., Berman, M., Switzer, P., & Craig, M. D. (1988). A Transformation for Ordering Multispectral Data in Terms of Image Quality with Implications for Noise Removal. *IEEE Transactions on Geoscience and Remote Sensing*, 26(1), 65–74. <https://doi.org/10.1109/36.3001>
- GSI. (2004). Kota Quadrangle. Retrieved May 19, 2017, from [http://www.portal.gsi.gov.in/pls/gsihub/PKG\\_PTL\\_SE\\_ARCH\\_PAGES.pGetImage\\_PaperMap?inpRecId=1344&nPaperMapImageId=PUB\\_PAPER\\_MAP](http://www.portal.gsi.gov.in/pls/gsihub/PKG_PTL_SE_ARCH_PAGES.pGetImage_PaperMap?inpRecId=1344&nPaperMapImageId=PUB_PAPER_MAP)
- Gupta, R. P. (2003). Introduction. In *Remote Sensing Geology* (2nd ed., pp. 1–16). New York: Springer- Verlag Berlin Heidelberg GmbH. <https://doi.org/10.1007/978-3-662-05283-9>
- Gupta, S. N., Arora, Y. K., Mathur, R. K., Iqballuddin, Prasad, B., Sahai, T. N., & Sharma, S. B. (1997). The Precambrian Geology of the Aravalli region, Southern Rajasthan & North-eastern Gujarat. *Memoir of the Geological Survey of India*, 123, 1–262.

- Harris, A. T. (2006). Spectral mapping tools from the Earth Sciences applied to Spectral Microscopy Data. *International Society for Analytical Cytology*, 69A(8), 872–879. <https://doi.org/10.1002/cyto.a.20309>
- Harris Geospatial Solutions. (2017). Continuum Removal. Retrieved June 10, 2017, from <https://www.harrisgeospatial.com/docs/ContinuumRemoval.html>
- Kruse, F. A. (1988). Use of airborne imaging spectrometer data to map minerals associated with hydrothermally altered rocks in the northern grapevine mountains, Nevada, and California. *Remote Sensing of Environment*, 24(1), 31–51. [https://doi.org/10.1016/0034-4257\(88\)90004-1](https://doi.org/10.1016/0034-4257(88)90004-1)
- Kruse, F. A. (1993). Artificial Intelligence for geologic mapping with Imaging Spectrometers Center for the Study of Earth from Space (CSES). United States.
- Kruse, F. A. (2002). Comparison of AVIRIS and Hyperion for Hyperspectral Mineral Mapping \*\*. In *Proceedings of the 11th JPL Airborne Geoscience Workshop*, JPL Publication.
- Kruse, F. A., Boardman, J. W., & Huntington, J. F. (2003). Comparison of Airborne Hyperspectral Data and EO-1 Hyperion for Mineral Mapping. *IEEE Transactions on Geoscience and Remote Sensing*, 41(6), 1388–1400. <https://doi.org/10.1109/TGRS.2003.812908>
- Kruse, F. A., Lefkoff, A. B., & Dietz, J. B. (1993). Expert System-Based Mineral Mapping in Northern Death Valley, California/Nevada, Using the Airborne Visible/Infrared Imaging Spectrometer (AVIRIS). *Remote Sensing of Environment*, 44(2–3), 309–336. [https://doi.org/10.1016/0034-4257\(93\)90024-R](https://doi.org/10.1016/0034-4257(93)90024-R)
- Rajesh, H. M. (2004). Application of Remote Sensing and GIS in mineral resource mapping - An overview. *Journal of Mineralogical and Petrological Sciences*, 99(3), 83–103. <https://doi.org/10.2465/jmps.99.83>
- Sabine, C. (1999). Strategies for Mineral Exploration. In A. N. Rencz & R. A. Ryerson (Eds.), *Manual of Remote Sensing: Remote Sensing for the Earth Sciences* (3rd ed., pp. 375–447). Canada: John Wiley & Sons, Inc.; American Society for Photogrammetry and Remote Sensing.
- Sabins, F. F. (1999). Remote sensing for mineral exploration. *Ore Geology Reviews*, 14(3–4), 157–183. [https://doi.org/10.1016/S0169-1368\(99\)00007-4](https://doi.org/10.1016/S0169-1368(99)00007-4)
- Swayze, G., Clark, R. N., Kruse, F., Sutley, S., & Gallagher, A. (1992). Ground-truthing AVIRIS mineral mapping at Cuprite, Nevada. In *JPL, Summaries of the Third Annual JPL Airborne Geoscience Workshop. Volume 1: AVIRIS Workshop* (pp. 47–49). United States: JPL Publication.
- Van der Meer, F. (2004). Analysis of spectral absorption features in Hyperspectral Imagery. *International Journal of Applied Earth Observation and Geoinformation*, 5(1), 55–68. <https://doi.org/10.1016/j.jag.2003.09.001>
- Van der Meer, F. D., Van Der Werff, H. M. A., Van Ruitenbeek, F. J. A., Hecker, C. A., Bakker, W. H., Noomen, M. F., ... Woldai, T. (2012). Multi- and hyperspectral geologic remote sensing: A review. *International Journal of Applied Earth Observations and Geoinformation*, 14(1), 112–128. <https://doi.org/10.1016/j.jag.2011.08.002>
- Van der Meer, F., & De Jong, S. (2003). Spectral Mapping Methods: Many Problems, Some Solutions. In *3rd EARSeL Workshop on Imaging Spectroscopy* (pp. 146–162). Hersching. Retrieved from [https://www.itc.nl/library/Papers\\_2003/peer\\_ref\\_conf/vandermeer\\_spectral.pdf](https://www.itc.nl/library/Papers_2003/peer_ref_conf/vandermeer_spectral.pdf)
- Verdel, C. S., Knepper, D., Livo, K. E., McLemore, V. T., Penn, B., & Keller, R. (2001). Mapping minerals at the copper flat porphyry using AVIRIS data. In *Proceedings of the 10th JPL Airborne Earth Sciences Workshop*, (pp. 427–433). New Mexico.